

НАЦИОНАЛЬНАЯ АКАДЕМИЯ НАУК УКРАИНЫ

МОРСКОЙ ГИДРОФИЗИЧЕСКИЙ ИНСТИТУТ



**СИСТЕМЫ КОНТРОЛЯ
ОКРУЖАЮЩЕЙ СРЕДЫ**

Сборник научных трудов

Севастополь
2002

Effect of the floating broken ice on the interaction of surface waves of finite amplitude

A.E. Bukatov, A.A. Bukatov

Marine Hydrophysical Institute of the Ukrainian
National Academy of Sciences
2, Kapitanskaja Str., Sevastopol 335000,
Ukraine
E-mail: ocean@alpha.mhi.iuf.net

ABSTRACT

The interaction of the propagating periodic surface waves of finite amplitude over the plane bottom in homogeneous fluid covered by floating broken ice is considered. The dependence of spatial profile of the basin's surface elevation, fluid particle transitional horizontal movement velocity, and total mean mass transport on the ice thickness and interacted harmonic parameters is investigated.

KEY WORDS

Wave interaction, ice effect, Stokes' drift, mass' transport.

INTRODUCTION

The propagation of the surface gravity waves of small amplitude in homogeneous fluid covered by floating ice was investigated by Peters (1950), Weitz and Keller (1950), Kheisin (1967), Bukatov (1970), Bukatov and Cherkessov (1971), Wadhams (1986). The non-linear wave propagation under the ice field was considered by Il'ichev and Marchenko (1989) in the case of shallow-water, and by Bukatov and Bukatova (1993) for the basin of constant finite depth.

The liquid particle stationary transport in the direction of the movement of periodic waves predicted by theory by Stokes (1847) was considered by Nesterov (1968), Newman (1985), Longuet-Higgins (1987) under the deep-water assumption, and by Sretenskii (1936), Phillips (1977), Aleshkov (1981), and Longuet-Higgins (1988) for the basin of finite depth. The influence of floating broken ice on the non-linear mass transport caused by propagating periodic wave in the fluid of finite depth was investigated by Bukatov and Bukatov (1999).

In this paper we consider the influence of floating broken ice on the non-linear interaction of periodic propagating waves of the first and second harmonics in the homogeneous fluid of constant finite depth. We use the method of multiple scales to obtain the

asymptotic expansions defining the fluid movement velocity potential and basin's surface elevation up to values of the third approximation order. Involving the Lagrange's coordinates we obtain the expressions for the transitional horizontal particle movement velocity and total mean mass transport. We study the dependence of the spatial profile of the basin's surface elevation and Stokes' drift velocity on the ice thickness and parameters of interacting harmonics. We estimate the ice effect on the range of the second harmonic amplitude satisfying the condition of consistency, and on the interval of the frequency shift.

PROBLEM STATEMENT

Let us consider a basin unbounded in horizontal directions and of constant depth H . This basin is filled with inviscous incompressible fluid. Its surface is covered by floating broken ice. We study influence of the ice on the non-linear interaction of propagating periodic waves of the first and second harmonics, assuming the friction of floating floes to be negligible. We also assume that the floes' sizes are small in comparison with the wavelengths, and oscillations of the floes are non-separating. Under mentioned assumptions, the floes' bend does not occur. In this connection, we take into account the gravity force as a single restoring force. Introduce the dimensionless variables $x = kx_1$, $z = kz_1$, $t = \sqrt{kg}t_1$ where k is the wavenumber. Then in the case of potential movement of the fluid, we have the following problem:

$$\Delta\varphi = 0, -\infty < x < \infty, -H < z < \zeta \quad (1)$$

with boundary conditions at the surface ($z = \zeta$)

$$\zeta - \frac{\partial\varphi}{\partial t} + \kappa k \frac{\partial^2\zeta}{\partial t^2} + \frac{1}{2} \left[\left(\frac{\partial\varphi}{\partial x} \right)^2 + \left(\frac{\partial\varphi}{\partial z} \right)^2 \right] = 0 \quad (2)$$

and at the basin's bottom ($z = -H$)

$$\frac{\partial\varphi}{\partial z} = 0 \quad (3)$$

At the initial moment ($t = 0$)

$$\zeta = f(x), \frac{\partial\zeta}{\partial t} = 0 \quad (4)$$

Here $\kappa = h\rho_1/\rho$, h and ρ_1 are thickness and density of the ice, ρ is the fluid density, g is the acceleration of gravity. The velocity potential φ and basin's surface elevation ζ are connected via the kinematic relation

$$\frac{\partial \zeta}{\partial t} - \frac{\partial \zeta}{\partial x} \frac{\partial \varphi}{\partial x} + \frac{\partial \varphi}{\partial z} = 0 \quad (5)$$

The term with multiplier κ in the dynamic condition (Eq. 2) represents the inertia of the ice vertical displacements. From Eq. 2 for $\kappa = 0$ there follows a dynamic condition on the open water..

EQUATIONS DEFINING THE NON-LINEAR APPROXIMATIONS

We find a solution to the problem defined by Eqs. 1-5 using the method of multiple scales (Nayfeh, 1976). Such a technique allows to obtain the uniformly converging expansions for ζ and φ . Let us introduce two new variables $T_1 = \varepsilon t$, $T_2 = \varepsilon^2 t$ which are changing slowly in comparison with $t = T_0$ where ε is small but finite. We assume

$$\{\zeta, \varphi, f\} = \sum_{n=1}^3 \varepsilon^n \{\zeta_n, \varphi_n, f_n\} + O(\varepsilon^4)$$

Here f_n are functions of x ; ζ_n are functions of x , T_j ; and φ_n are functions of x, z, T_j where $j = 0, 1, 2$.

Substituting these expansions into Eqs. 1-5 and setting the terms with same orders of ε to zero, we obtain (Bukatov, 1994) the appropriate equations for defining the approximations ζ_n and φ_n with orders ε^n , $n = 1, 2, 3$

$$\Delta \varphi_n = 0, -\infty < x < \infty, -H < z < \zeta \quad (6)$$

$$\zeta_n - \frac{\partial \varphi_n}{\partial T_0} + \kappa k \frac{\partial^2 \zeta_n}{\partial T_0^2} = P_n, z = 0 \quad (7)$$

$$\frac{\partial \zeta_n}{\partial T_0} + \frac{\partial \varphi_n}{\partial z} = L_n, z = 0 \quad (8)$$

$$\frac{\partial \varphi_n}{\partial z} = 0, z = -H \quad (9)$$

$$\zeta_n = f_n(x), \frac{\partial \zeta_n}{\partial T_0} = G_n, t = 0 \quad (10)$$

Expressions for P_n, G_n, L_n are given in Appendix 1.

DEFINITION OF VELOCITY POTENTIAL AND SURFACE ELEVATION

A problem defined by Eqs. 6-10 is written in general case of unsteady disturbances of finite amplitude. Here we consider only propagation of periodic waves by choosing $f_n(x)$ in appropriate forms.

We choose the first order approximation ($n = 1$) of the basin' surface elevation ζ_1 in the form

$$\zeta_1 = \cos \theta + a_1 \cos 2\theta, \theta = x + \tau T_0 + \beta_1(T_1, T_2) \quad (11)$$

where a_1 is a constant of the order of unit; $\beta_1(0) = 0$. Satisfying the boundary condition at the basin's bottom and taking into account correlation between the wave parameters via the boundary conditions at the basin's surface (Eqs. 7, 8), we write

$$\varphi_1 = \tau \left[\frac{\cosh(z+H)}{\sinh H} \sin \theta + a_1 \frac{\cosh 2(z+H)}{\sinh 2H} \sin 2\theta \right] \quad (12)$$

$$\tau^2 = \tau_0^{-1} \tanh H, \tau_0 = 1 + \kappa k \tanh H$$

We'll define the amplitude a_1 and the phase shift β_1 from the following approximations.

Substituting ζ_1, φ_1 form Eqs. 11, 12 into the right-hand sides of Eqs. 7 and 8 for the second-order approximation, and solving the problem defined by Eqs. 6-9 with $n = 2$ taking into account requirement of absence of the first and second harmonics in a particular solution, we obtain

$$\zeta_2 = a_2 \cos 2\theta + \sum_{n=3}^4 a_{2n} \cos n\theta \quad (13)$$

$$\varphi_2 = \tau^2 b_{20} t + \tau \sum_{n=1}^4 b_{2n} \cosh n(z+H) \sinh^{-1} nH \sin n\theta \quad (14)$$

$$a_1 = \pm \frac{1}{2} [\tau_0 \tau_*^{-1} \coth H \tanh 2H]^{1/2} \quad (15)$$

$$\tau_* = 1 + 2\kappa \tanh 2H, \beta_1 = \varepsilon \tau_1 t + \beta_2(T_2)$$

$$\tau_1 = \frac{a_1 \tau}{4\tau_0} (4 \coth 2H + \coth H - 3 \tanh H)$$

Expressions defining a_{23}, a_{24} and b_{2n} (where $n = 0, 1, \dots, 4$) are given in Appendix 2, and expressions for a_2 and β_2 may be obtained from the third-order approximation.

The expressions for ζ_1, φ_1 (Eqs. 11, 12) and for ζ_2, φ_2 (Eqs. 13, 14) define the right-hand sides of the dynamic (Eq. 7) and kinematic (Eq. 8) conditions with $n=3$. Excluding there the secular terms, we find

$$a_2 = \frac{1}{2} (\omega_2 - \delta) / \omega_1, \beta_2 = \varepsilon^2 \tau_2 t$$

$$\delta = \tau (\gamma_2 - q_2 \tanh 2H) / (4a_1 \tau_*)$$

$$\tau_2 = \omega_2 - \omega_1 a_2, \omega_1 = -\tau_1 / a_1, \omega_2 = \frac{1}{2} (\gamma_1 - q_1 \tanh H) \tau / \tau_0$$

and expressions defining $\gamma_1, \gamma_2, q_1, q_2$ are given in Appendix 3.

Now we may write the solution to the problem in the third-order approximation ($n = 3$) in the form

$$\zeta_3 = a_3 \cos 2\theta + \sum_{n=3}^6 a_{3n} \cos n\theta$$

$$\varphi_3 = \tau^2 b_{30} t + \tau \sum_{n=1}^6 b_{3n} \cosh n(z+H) \sinh^{-1} nH \sin n\theta \quad (16)$$

The expressions for a_{3n}, b_{3n} (where $n = 0, 1, 2, \dots, 6$) are given in Appendix 4, and a_3 may be defined from the equations for the fourth-order approximation.

Thus, we obtain the following expression up to the third-order approximation for the disturbance of the surface of the basin of finite depth covered by broken ice when the propagating periodic waves of two first harmonics are interacting:

$$\zeta = \varepsilon \cos \theta + \sum_{n=1}^3 \varepsilon^n a_n \cos 2\theta + \sum_{n=2}^3 \varepsilon^n \sum_{j=3}^4 a_{nj} \cos j\theta + \varepsilon^3 \sum_{n=5}^6 a_{3n} \cos n\theta$$

$$\theta = x + \sigma t, \sigma = \tau(1 + \varepsilon \sigma_1 + \varepsilon^2 \sigma_2), \sigma_1 = \tau_1/\tau, \sigma_2 = \tau_2/\tau$$

We define the wave disturbance phase velocity from the formula

$$v = \tau k^{-1} (1 + \varepsilon \sigma_1 + \varepsilon^2 \sigma_2).$$

Basing of Eqs. 12, 14 and 16, we may write the corresponding expression for the velocity potential in the form

$$\varphi = \varepsilon \varphi_1 + \varepsilon^2 \varphi_2 + \varepsilon^3 \varphi_3$$

The expression for the basin's surface elevation in dimensional variables ($x = x/k, t = t/\sqrt{kg}$, $\zeta = \zeta/k, a = \varepsilon/k$ where a is an initial value of the main harmonic amplitude) may be written as

$$\zeta = a \zeta_1 + a^2 k \zeta_2 + a^3 k^2 \zeta_3$$

In this connection,

$$\theta = kx + \sigma t, \sigma = \tau \sqrt{kg} (1 + ak\sigma_1 + a^2 k^2 \sigma_2)$$

$$v = \tau \sqrt{g/k} (1 + ak\sigma_1 + a^2 k^2 \sigma_2).$$

ANALYSIS OF THE WAVE CHARACTERISTICS

It follows from the obtained expressions that the frequency σ and phase velocity v depend not only on the ice thickness but also on the amplitudes of interacting harmonics. In this connection, the influence of amplitudes in the ice-covered basin and basin with open water manifests itself both in the second- and first-order approximations. If $a_1 = 0$ then the wave frequency and phase velocity in the ice-

covered basin and basin with open water depend on the initial harmonic amplitude in the second-order approximation only. It is seen from Eq. 15 that the amplitude a_1 of the second initial harmonic may change between $1/2$ and $1/\sqrt{2}$ when the ice is absent. Its value for the ice-covered basin varies within the range from $1/(2\sqrt{2})$ to $1/\sqrt{2}$. The value of a_1 may be found under the deep-water (a_1^d) and shallow-water assumption (a_1^s) as

$$a_1^d = \pm \frac{1}{2} \sqrt{\frac{1 + \kappa k}{1 + 2\kappa k}}, a_1^s = \pm \frac{1}{\sqrt{2}} \sqrt{\frac{1 + \kappa k^2 H}{1 + 4\kappa k^2 H}}.$$

Under the same conditions, the expressions for $\sigma_0 = \tau \sqrt{kg} \sigma_1$ defining the oscillation phase shift in the approximation of the order of ε may be written in the form

$$\sigma_0^d = \pm \frac{1}{4(1 + \kappa k)} \sqrt{\frac{kg}{1 + 2\kappa k}}$$

$$\sigma_0^s = \pm \frac{3 - (kH)^2}{4(1 + \kappa k^2 H)} \sqrt{\frac{g}{2H(1 + 4\kappa k^2 H)}}.$$

The direction of this phase shift is defined by the sign by a_1 .

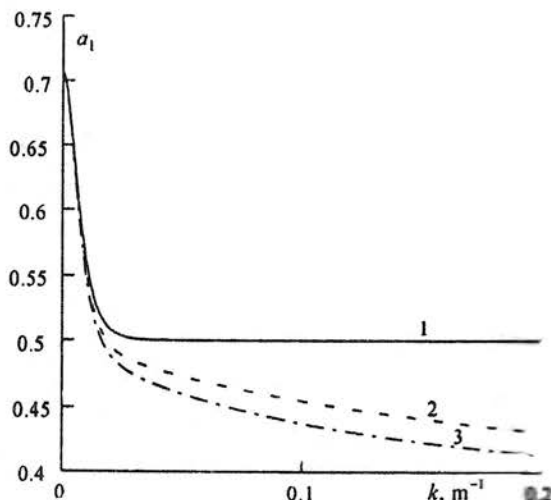


Fig. 1. Initial amplitude of the second harmonic as a function of the wave number in the cases $h = 0$ (line 1), $h = 3m$ (line 2), and $h = 5m$ (line 3).

In order to estimate the dependence of the wave disturbance on the ice conditions and parameters of interacting harmonics, we carried out the numerical computations for

$$H=100m, 0 \leq h \leq 5m, \rho_1/\rho=0.87 \quad (17)$$

Our analysis showed that the second harmonic initial amplitude a_1 decreases with increasing ice thickness and decreasing the interacting harmonic wavelengths. It is seen on the plots of a_1 as functions of the wave number k in Fig.1. Here the lines 1, 2, and 3 correspond to the ice thickness 0, 3, and 5m. The change in the second harmonic initial phase to its opposite deforms the spatial profile of the basin's surface disturbances both quantitatively and qualitatively. This may be seen by comparing the profiles of $\zeta(x)$ showed in Figs.2 and 4 for $a_1 > 0$ with ones in Figs. 3 and 5 for $a_1 < 0$.

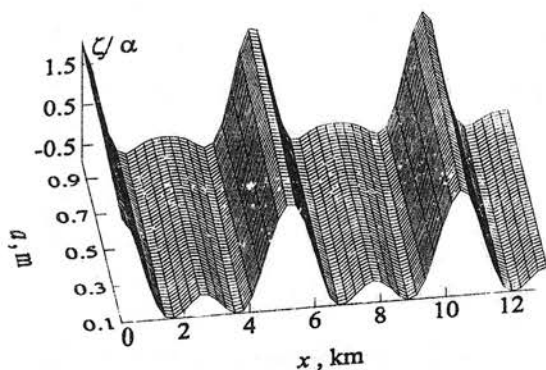


Fig.2. The wave profiles along the x -axis as functions of the main harmonic amplitude for $\lambda=5\pi/3 \cdot 10^3 m$, $h=0$, $t=0$ in the case $a_1 > 0$.

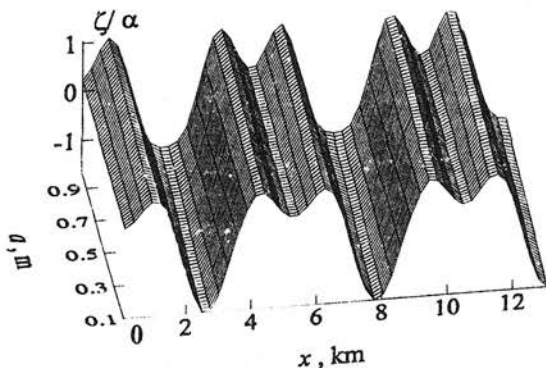


Fig.3. The same as in Fig.2, in the case $a_1 < 0$. $1.2 \cdot 10^{-4} \leq \varepsilon \leq 1.2 \cdot 10^{-3}$

The illustrations are given in Figs.2 and 3 for $kH=0.12$, $1.2 \cdot 10^{-4} \leq \varepsilon \leq 1.2 \cdot 10^{-3}$, and for $\varepsilon=10^{-3}$, $0.1 \leq kH \leq 0.2$ in Figs. 4 and 5 in the case $t=0$, $h=0$. The mentioned ε and k correspond to the following values of the wave amplitude a and the wavelength λ of the initial harmonic:

$$0.1m \leq a \leq 1m, \lambda=5\pi/3km \quad (\text{Figs.2 and 3}) \quad \text{and}$$

$$0.5m \leq a \leq 1m, 10\pi \leq \lambda/H \leq 20\pi \quad (\text{Figs.4 and 5}).$$

It is seen that the maximal vertical deviations of the basin's surface are displayed as the peaks and troughs in the cases $a_1 > 0$ and $a_1 < 0$, respectively.

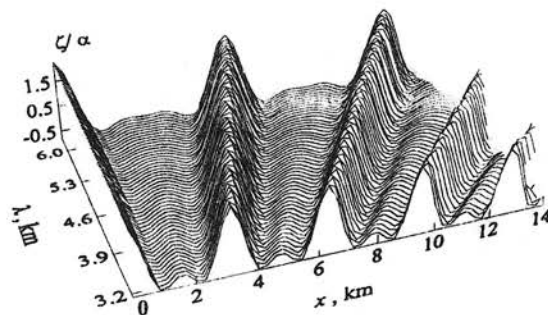


Fig.4. The wave profiles along the x -axis as functions of the main harmonic wavelength for $\varepsilon=10^{-3}$, $h=0$, $t=0$ in the case $a_1 > 0$.

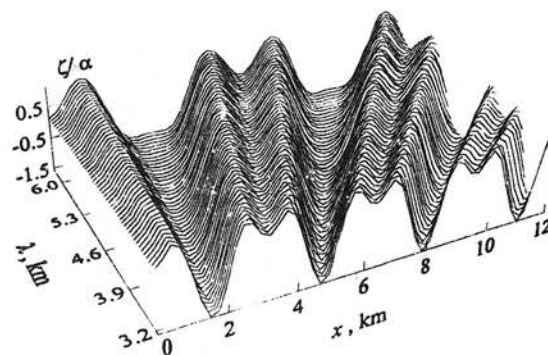


Fig.5. The same as in Fig.4, in the case $a_1 < 0$.

The increasing t results in the disturbance phase shift. The direction of the horizontal deviation in the wave disturbance spatial profile with time coincides with the direction of the propagation of this disturbance. In the case $\varepsilon=10^{-3}$, $kH=0.1$, $h=0$, such deviations are shown in Fig. 6 for $a_1 > 0$ and Fig. 7 for $a_1 < 0$. The plots for $t=0$ are shown by the lines 1 in both Figures. The lines 2 correspond to $t=60s$ in Fig.6 and $t=30s$ in Fig.7.

Remind that we consider the waves propagating in the opposite x -direction.

The oscillation phase shift occurs also with increasing ice thickness. This effect amplifies with time. The larger the initial harmonic wavelength the later (in time) such phase shifts manifest. In particular, in the case $\varepsilon=10^{-3}$, $kH=0.1$, they become noticeable only for $t > 10$ hours, although for $\varepsilon=10^{-1}$, $kH=10$ they appear already when $t > 10$ seconds. The direction of the phase shift caused by

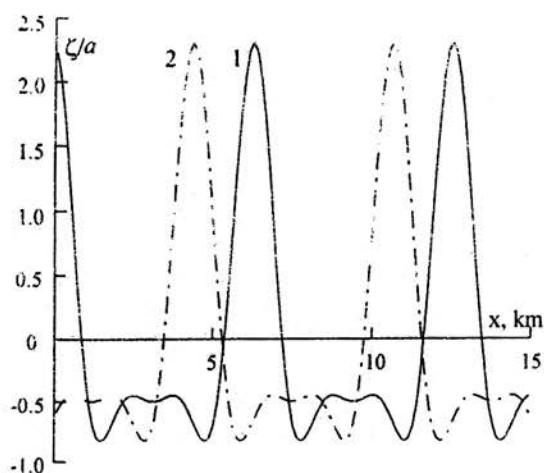


Fig.6. Surface elevation for $t = 0$ (line 1) and $t = 60s$ (line 2) in the case $a_1 > 0$, $h = 0$. Here the main harmonic wavelength and amplitude are $\lambda = 2\pi \cdot 10^3 m$ and $a = 1 m$.

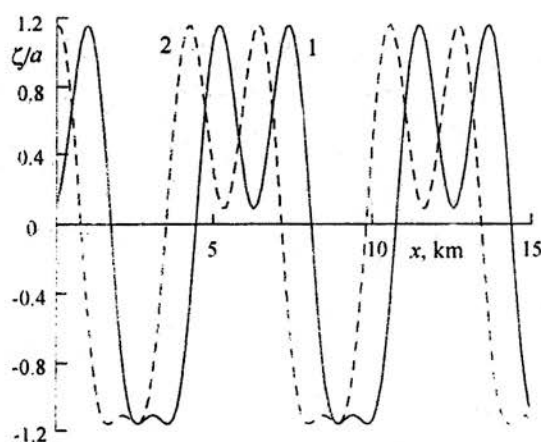


Fig.7. Surface elevation for $t = 0$ (line 1) and $t = 30s$ (line 2) in the case $a_1 < 0$, $h = 0$. Here the main harmonic wavelength and amplitude are $\lambda = 2\pi \cdot 10^3 m$ and $a = 1 m$.

ice effect does not change when the second harmonic initial phase (or the sign by a_1) changes to its opposite. In this connection, in the case $a_1 < 0$, the effects both of the ice and of the non-linearity lead to decrease in the initial frequency of the oscillations (and decrease in the wave disturbance propagation phase velocity). If $a_1 > 0$ then the ice effect results in decrease, and non-linearity effect results in increase in the velocity of the disturbance spatial profile displacement. In such a case, under the deep-water approximation, the non-linearity effect is stronger than the ice effect when the wave number k is less than $\varepsilon/(2\kappa)$. If $k > \varepsilon/(2\kappa)$, the opposite phenomenon occurs.

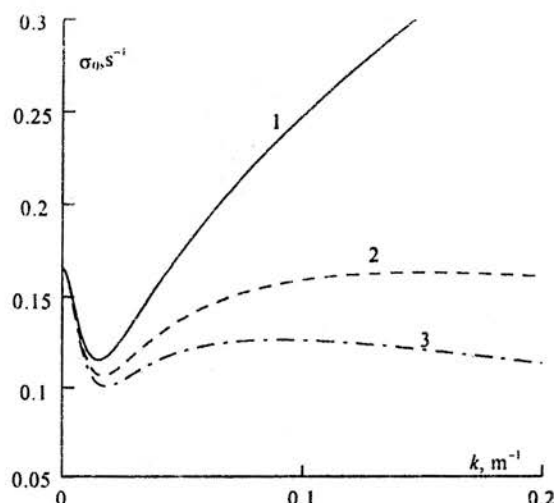


Fig.8. Frequency shift in the ε -order approximation as a function of the wave number for $h = 0$ (line 1), $h = 3m$ (line 2), and $h = 5m$ (line 3).

Under the shallow-water approximation, the ice effect is stronger than the effect of the non-linearity when $k > k_0$ where $k_0 = [3\varepsilon(2\sqrt{2}\kappa H^2)^{-1}]^{1/3}$. If

$k > k_0$ then the effect of the non-linearity accelerates the waves stronger than the ice effect brakes them. The influence of the ice on the frequency shift in the approximation of the first order of ε is shown on the plots in Fig.8. In Fig.9 we showed a_1 versus σ_0 . In both Figures, the curves $\sigma_0(k)$ and $a_1(\sigma_0)$ with numbers 1, 2, and 3 correspond to the ice thickness being equal to 0, 3, and 5m. The point I in Fig.9 denotes value of a_1 for $\sigma_0(0) = 3/4(g/2H)^{1/2}$. The points II and III denote a_1 corresponding to the local maximum and local minimum of $\sigma_0(k)$.

Under the deep-water approximation when $h \neq 0$, the local maximum of $\sigma_0(k)$ is achieved for $k = (\sqrt{17} - 1)(8\kappa)^{-1}$. Its value is

$$\sigma_0^{\max} = \frac{2\sqrt{g}}{7 + \sqrt{17}} \sqrt{\frac{\sqrt{17} - 1}{2\kappa(3 + \sqrt{17})}}$$

and limits the range of the frequency shift (in the approximation of the first order of ε) from above. This value decreases with increasing ice thickness. There are values of σ_0 in whose the amplitude $a_1(\sigma_0)$ of the second interacting harmonic may have three different values (see Fig.9). The function $\sigma^*(k) = \tau\sqrt{kg}\sigma_2$ characterizing the frequency shift in the ε^2 -order approximation, and the function $a_1(\sigma^*)$, have the same features.

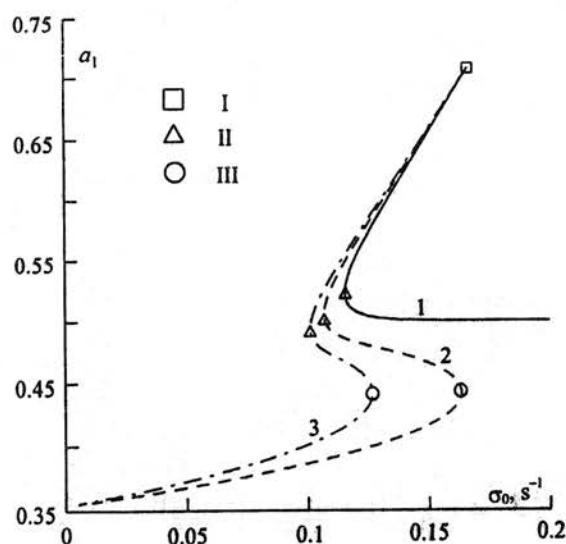


Fig.9. Initial amplitude of the second harmonic as a function of the frequency shift in the ε -order approximation for $h = 0$ (line 1), $h = 3m$ (line 2), and $h = 5m$ (line 3).

In the case of short waves, the ice effect manifests itself not only in the decrease in the phase velocity but also in the weak decrease in the wave heights. In this connection, the last effect is stronger when $a_1 > 0$ than in the case $a_1 < 0$. This may be seen by comparing the plots in Fig.10 (for $a_1 > 0$) and in Fig.11 (for $a_1 < 0$). These plots are given for $\varepsilon = 10^{-1}$, $kH = 10$, $t = 15s$. The lines 1 in both Figures characterize disturbances of the basin with open water ($h = 0$). The lines 2 correspond to $h = 3m$ in Fig.10, and $h = 5m$ in Fig.11.

Remind that the value of a_3 , being of the same order as the a_{3n} ($n = 3 + 6$) and determining along with them the solution in the third-order approximation, may be found from the fourth-order approximation only.

Therefore, this value was not taken into consideration in the numerical calculation of the $\zeta(x)$ profiles. However, in order to estimate tentatively the error (in the quantity of the third-order contribution) admitted in this way, computations were carried out for both $a_{3n} = 0$ and $a_{3n} \neq 0$. A comparison of the results obtained did not establish fundamental quantitative differences between them. Ignoring the quantities a_{3n} leads only to an insignificant decrease in the extreme values of ζ and to only a slight flattening of the tops of the peaks and the bottom of the troughs, this effect decreasing with decrease in the initial harmonic wavelengths.

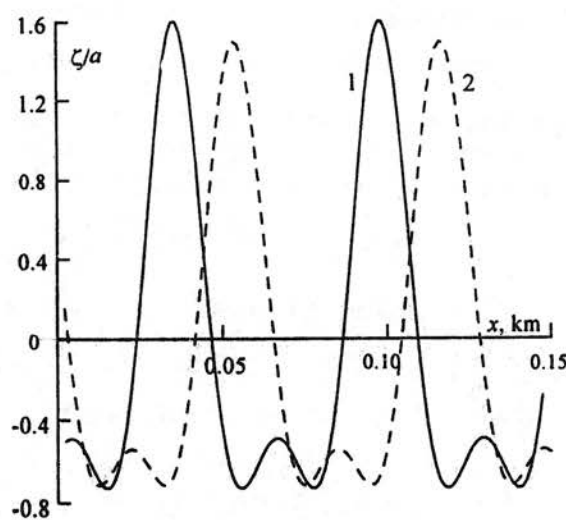


Fig.10. Surface elevation for $h = 0$ (line 1) and $h = 3m$ (line 2) in the case $a_1 > 0$, $t = 15s$. Here the main harmonic wavelength and amplitude are $\lambda = 20\pi m$ and $a = 1m$.

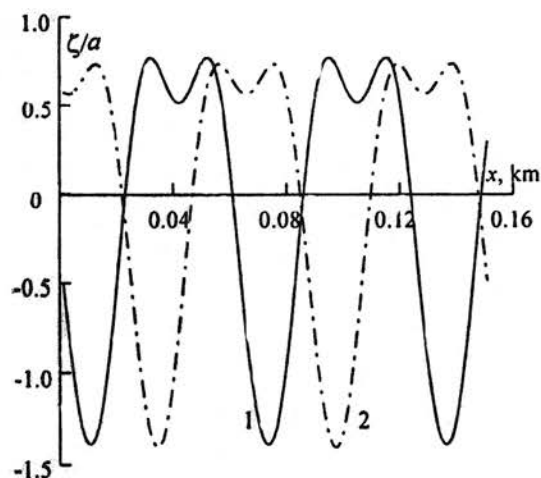


Fig.11. Surface elevation for $h = 0$ (line 1) and $h = 5m$ (line 2) in the case $a_1 < 0$, $t = 15s$. Here the main harmonic wavelength and amplitude are $\lambda = 20\pi m$ and $a = 1m$.

MASS' TRANSPORT

Following Newman (1985), we can describe the orbital movement of a fixed liquid particle with using the Lagrange's coordinates defining its position.

It can be shown that the liquid particle vertical displacement is periodic with the velocity

$$w = \sum_{n=1}^3 \varepsilon^n \partial \varphi_n / \partial z \text{ up to quantities of the fourth order}$$

of ε . The expression defining the horizontal velocity of the particle displacement $u = \sum_{n=1}^3 \varepsilon^n \partial \varphi_n / \partial x$ contains not only a periodic component but also a Stokes' steady transitional displacement velocity which may be written in this case in the form

$$u_0 = -\varepsilon^2 \frac{g\tau}{\sqrt{kg}} A_1 (1 - \varepsilon A_0 - \varepsilon^2 A) + O(\varepsilon^5) \quad (18)$$

$$A_0 = \sigma_1 - (A_2 - C) A_1^{-1}$$

$$A = \sigma_2 + [F - D + \sigma_1 (A_2 - 2C)] A_1^{-1}$$

$$A_1 = \sum_{n=1}^2 A_{1n} \sinh^{-2} nH \cosh 2n(z+H), i=1, 2$$

$$A_{11} = \frac{1}{2}, A_{12} = 2a_1^2, A_{21} = b_{21}, A_{22} = 4a_1 b_{22}$$

$$C = a_1 F_1 C_1, D = \sum_{n=1}^4 D_n \sinh^{-2} nH \cosh 2n(z+H)$$

$$F = F_1 C_1 (b_{22} + 2b_{21} a_1) + 8b_{24} a_1^2 F_2 C_2 +$$

$$+ \frac{1}{2} a_1 b_{23} F_0 \prod_{n=1}^3 \sinh^{-1} nH$$

$$C_j = 4 \cosh 4j(z+H) - \cosh 2j(z+H)$$

$$F_j = \frac{1}{4} \sinh^{-2} jH \sinh^{-1} 2jH, j=1, 2$$

$$F_0 = \frac{27}{2} \cosh 6(z+H) - 4 \cosh 4(z+H) - \frac{1}{2} \cosh 2(z+H)$$

$$D_1 = b_{31} + \frac{1}{2} b_{21}^2, D_2 = 4a_1 b_{32} + 2b_{22}^2$$

$$D_3 = \frac{9}{2} b_{23}^2, D_4 = 8b_{24}^2$$

If $z=0$ and $\kappa \neq 0$, u_0 characterizes velocity of the ice Stokes' drift under conditions of non-linear interaction of periodic propagating waves of the first and second harmonics.

It should be noted that the expression defining the velocity of the mass' transport by a propagating wave in fluid of finite depth with open surface given by Sretenskii (1936), Phillips (1977), Aleshkov (1981), may be obtained by restricting Eq. 21 to the quantities up to the second order of ε in the case $a_1=0$, $h=0$. Under such assumptions, the mass' transport quantity is in agreement with the results by Longuet-Higgins (1987, 1988).

Integration of Eq. 18 over the vertical coordinate z yields the total mean mass' transport in the direction of propagation of the wave harmonics

$$Q = \varepsilon^2 \frac{g\tau}{k\sqrt{kg}} (Q_0 + \varepsilon Q_1 + \varepsilon^2 Q_2) \quad (19)$$

$$Q_0 = \frac{1}{2} \coth H + a_1^2 \coth 2H, Q_2 = Q_{21} - Q_{22}$$

$$Q_1 = \sum_{n=1}^2 B_{1n} \coth nH - \frac{1}{2} a_1 \left(\frac{5}{4} + \frac{3}{4} \coth^2 H \right)$$

$$Q_{21} = \sum_{n=1}^2 \left[B_{2n} \left(\frac{5}{4} + \frac{3}{4} \coth^2 nH \right) - B_{3n} \coth nH \right] +$$

$$+ \sum_{n=1}^4 \frac{1}{n} D_n \coth nH$$

$$Q_{22} = \frac{1}{8} a_1 b_{23} (9 \sinh 6H - 4 \sinh 4H -$$

$$- \sinh 2H) \prod_{n=1}^3 \sinh^{-1} nH$$

$$B_{11} = b_{21} - \frac{1}{2} \sigma_1, B_{12} = a_1 (2b_{22} - \sigma_1 a_1),$$

$$B_{21} = a_1 (\sigma_1 - b_{21}) - \frac{1}{2} b_{22}, B_{22} = -2a_1^2 b_{24}$$

$$B_{31} = \sigma_1 b_{21} + \frac{1}{2} \sigma_2, B_{32} = a_1 (2\sigma_1 b_{22} + a_1 \sigma_2)$$

It follows from Eqs. 18 and 19 that the main approximations to the particle transitional movement velocity are magnitudes of the second order of smallness. They do not depend on the initial phase of the second interacting harmonic and decrease with increasing ice thickness. Their values exceed those for the case of propagating non-linear surface wave ($a_1=0$) when other conditions are the same. Besides, if $a_1 \neq 0$ then the magnitudes of the third and fourth orders of smallness introduce their contributions to u_0 and Q , too. If $a_1=0$, the terms of the third order are absent in u_0 and Q .

In order to estimate the transitional movement velocity of the liquid particles at the basin's surface and total mean mass' transport in the fluid, as well as their dependence on the ice thickness and parameters of the interacting harmonics, we carried out (Bukatov and Bukatov, 2001) a numerical analysis basing on Eqs. 18, 19 and parameter values from Eq. 17.

The main harmonic wavelength $\lambda = 2\pi/k$ changed within the range $0.2\pi H \leq \lambda \leq 20\pi H$.

Note that the term of the fourth order of smallness in Eq. 21 for the liquid particle transitional movement velocity depends on the quantity a_3 which is one of three terms of the same order in the expression for a_{32} . In our computations, a_3 was assumed to be equal to zero because it may be defined only from the equation for the fourth-order approximation. However, in order to estimate tentatively the error introduced in this manner, we computed the Stokes' drift velocity both for $a_{32}=0$ and for $a_{32} \neq 0$. The comparison of the obtained

results showed that a mistake caused by neglect of a_{32} is less than one percent.

The obtained results show that the liquid particle transitional movement velocity and total mean mass' transport in the direction of propagation of the interacting harmonics in the ice-covered basin are less than in the basin with open water. These differences increase with increasing ice thickness and harmonic amplitudes but decrease with increasing wavelength λ of the main harmonic. In particular, when $\lambda = 62.8m$, the values of $U = -u_0(0)$ and Q decrease by 33.3 and 27.8%, respectively with h changing from 0 to 5m, if $a = 1m$, and by 29.9 and 25.1%, respectively, if $a = 0.5m$. For $\lambda = 125.6m$, the same change in h leads to decrease in U and Q by 19.4 and 16%, when $a = 1m$, and by 17.8 and 15%, when $a = 0.5m$.

Being involved into the formation of the wave disturbances, the second interacting harmonic increase the liquid particle transitional movement velocity and total mean mass' transport. However, the change in U and Q caused by the second harmonic becomes weaker with increasing ice thickness. For example, for $a = 1m$ and $\lambda = 62.8m$, the values of U and Q in the case $a_1 \neq 0$ are greater than if $a_1 = 0$ by 85.5 and 35.8%, respectively, when $h = 0$, and by 47.9 and 17.2%, respectively, when $h = 5m$.

CONCLUSIONS

When there occurs non-linear interaction of the wave harmonics of finite amplitude, the disturbance frequency depends on the main harmonic initial amplitude not only in the second- but also in the first-order approximation. In this connection, in the first-order approximation, the range of variation of the phase shift is bounded above because of the ice effect.

The influence of the ice may appear in the case of interaction of short waves as well as in the case of interaction of long ones. In the last case it manifests itself mainly in the phase shift of the wave disturbance spatial distribution. This shift increases with time. The longer the initial main harmonic wavelength the later the phase shift appears. In the case of short waves, the noticeable ice effect manifests itself in the decrease not only in the phase velocity but also in the disturbance amplitude. In this connection, the decrease in the amplitude is more appreciable when the initial phases of interacted harmonics coincide at the origin than in the case when their phases are opposite.

The change in the phase of the second initial harmonic to its opposite leads to both quantitative and qualitative deformations of the profile of the

disturbance spatial distribution. In this connection, the direction of the phase variation caused by the ice does not change.

The contribution of the second interacting harmonic in the formation of the wave disturbances leads to the increase in the non-linear mass transport. The floating broken ice decreases the transitional velocity of the liquid particles and total mean mass transport. The ice effect amplifies with increasing steepness of the initial harmonic wave. The thicker the ice the lower its Stokes' drift velocity.

Appendix 1. Expressions for P_n, G_n, L_n .

$$P_1 = L_1 = G_1 = 0$$

$$P_2 = \zeta_1 \frac{\partial^2 \varphi_1}{\partial T_0 \partial z} + \frac{\partial \varphi_1}{\partial T_1} - \frac{1}{2} \left[\left(\frac{\partial \varphi_1}{\partial x} \right)^2 + \left(\frac{\partial \varphi_1}{\partial z} \right)^2 \right] - 2\kappa k \frac{\partial^2 \zeta_1}{\partial T_0 \partial T_1}$$

$$L_2 = \frac{\partial \zeta_1}{\partial x} \frac{\partial \varphi_1}{\partial x} - \frac{\partial \zeta_1}{\partial T_1} - \zeta_1 \frac{\partial^2 \varphi_1}{\partial z^2}, G_2 = -\frac{\partial \zeta_1}{\partial T_1}$$

$$P_3 = \zeta_1 N_1 + \frac{1}{2} \zeta_1^2 \frac{\partial^3 \varphi_1}{\partial T_0 \partial z^2} + \zeta_2 \frac{\partial^2 \varphi_1}{\partial T_0 \partial z} + \frac{\partial \varphi_2}{\partial T_1} + \frac{\partial \varphi_1}{\partial T_2} - \frac{\partial \varphi_1}{\partial x} \frac{\partial \varphi_2}{\partial x} - \frac{\partial \varphi_1}{\partial z} \frac{\partial \varphi_2}{\partial z} - \kappa k N_2$$

$$N_1 = \frac{\partial^2 \varphi_1}{\partial T_1 \partial z} + \frac{\partial^2 \varphi_2}{\partial T_0 \partial z} - \frac{\partial \varphi_1}{\partial x} \frac{\partial^2 \varphi_1}{\partial z \partial x} - \frac{\partial \varphi_1}{\partial z} \frac{\partial^2 \varphi_1}{\partial z^2}$$

$$N_2 = \frac{\partial^2 \zeta_1}{\partial T_1^2} + 2 \frac{\partial^2 \zeta_2}{\partial T_0 \partial T_1} + 2 \frac{\partial^2 \zeta_1}{\partial T_0 \partial T_2}$$

$$L_3 = \zeta_1 \left(\frac{\partial \zeta_1}{\partial x} \frac{\partial^2 \varphi_1}{\partial x \partial z} - \frac{\partial^2 \varphi_2}{\partial z^2} \right) - \frac{1}{2} \zeta_1^2 \frac{\partial^3 \varphi_1}{\partial z^3} - \zeta_2 \frac{\partial^2 \varphi_1}{\partial z^2} + N_3, G_3 = -\frac{\partial \zeta_1}{\partial T_2} - \frac{\partial \zeta_2}{\partial T_1}$$

$$N_3 = \frac{\partial \zeta_2}{\partial x} \frac{\partial \varphi_1}{\partial x} + \frac{\partial \zeta_1}{\partial x} \frac{\partial \varphi_2}{\partial x} - \frac{\partial \zeta_1}{\partial T_2} - \frac{\partial \zeta_2}{\partial T_1}$$

Appendix 2.

$$a_{2n} = -a_1 \tau^2 F_n \mu_n^{-1}, n = 3, 4,$$

$$\mu_n = (1 - n^2 \kappa k \tau^2) \tanh nH - n\tau^2$$

$$F_3 = \frac{1}{2} [3(2 \coth 2H + \coth H) + (2 \coth H \coth 2H - 7) \tanh 3H]$$

$$F_4 = [4 \coth 2H + (\coth^2 2H - 3) \tanh 4H] a_1$$

$$b_{20} = \frac{1}{4} [\coth^2 H - 1 - 4a_1^2 (1 - \coth^2 2H)]$$

$$b_{21} = -\frac{1}{2} a_1 (2 \coth 2H + \coth H) + \sigma_1, \quad b_{22} = a_2 + a_0$$

$$b_{23} = a_{23} - \frac{1}{2} (2 \coth 2H + \coth H) a_1$$

$$b_{24} = a_{24} - a_1^2 \coth 2H, \quad a_0 = a_1 \sigma_1 - \frac{1}{2} \coth H$$

Appendix 3.

$$\gamma_1 = \frac{1}{2} a_1 (b_{21} \coth H + 3b_{23} \coth 3H) +$$

$$+ (a_0 + a_1 a_{23}) \coth 2H + \frac{9}{4} a_1^2 + \frac{3}{8}$$

$$\gamma_2 = (b_{21} + a_{23}) \coth H + 3(b_{23} \coth 3H + a_1^3)$$

$$+ a_1 (2a_{24} \coth 2H + 4b_{24} \coth 4H + 3)$$

$$q_1 = \sum_{n=1}^3 q_{1n}, \quad q_2 = \sum_{n=1}^3 q_{2n},$$

$$q_{11} = a_1 \left(\frac{5}{2} \sigma_1 - \frac{1}{2} b_{21} + 2a_{23} \right) + a_0 + \kappa \kappa \sigma_1^2$$

$$q_{12} = \left(\sigma_1 b_{21} - \frac{7}{4} a_1^2 - \frac{5}{8} \right) \coth H - 5a_1^2 \coth 2H$$

$$q_{13} = a_1 b_{23} \left(\frac{3}{2} - 3 \coth 2H \coth 3H \right) -$$

$$- (a_0 + a_1 b_{21}) \coth H \coth 2H$$

$$q_{21} = (2a_0 \sigma_1 - 5a_1^3 + a_1) \coth 2H - \frac{5}{2} a_1 \coth H$$

$$q_{22} = 4a_1 b_{24} (1 - \coth 2H \coth 4H) + b_{21} \left(1 - \frac{1}{2} \coth^2 H \right)$$

$$+ \frac{3}{2} b_{23} (2 - \coth H \coth 3H)$$

$$q_{23} = 2a_1 (a_{24} + 2\kappa \kappa \sigma_1^2) + \frac{1}{2} (a_{23} + \sigma_1)$$

Appendix 4.

$$a_{3n} = \tau^2 (q_n \tanh nH - \gamma_n) \mu_n^{-1}, \quad n = 3, 4, 5, 6$$

$$\gamma_3 = \gamma_{31} + \gamma_{32}, \quad \gamma_{31} = \frac{27}{8} a_1^2 - 3a_{23} \sigma_1 + \frac{3}{8}$$

$$\gamma_{32} = \frac{3}{2} (b_{21} a_1 + a_2 + a_{24}) \coth H +$$

$$+ 3(a_0 + a_2) \coth 2H + 6b_{24} \coth 4H$$

$$\gamma_4 = 2a_{23} \coth H + a_1 [4(2a_2 + a_0) \coth 2H + 3] +$$

$$+ 6b_{23} \coth 3H - 4a_{24} \sigma_1$$

$$\gamma_5 = a_1 \left(5a_{23} \coth 2H + \frac{15}{2} b_{23} \coth 3H \right) +$$

$$+ \frac{5}{2} a_{24} \coth H + 10b_{24} \coth 4H + \frac{45}{8} a_1^2$$

$$\gamma_6 = a_1 (6a_{24} \coth 2H + 12b_{24} \coth 4H) + 3a_1^3$$

$$q_3 = \sum_{n=1}^3 q_{3n}, \quad q_4 = \sum_{n=1}^2 q_{4n}, \quad q_5 = \sum_{n=1}^2 q_{5n}$$

$$q_6 = a_1 [4b_{24} (3 - \coth 2H \coth 4H) + a_1^2 \coth 2H + 2a_{24}]$$

$$q_{31} = a_2 \left(\frac{7}{2} - \coth H \coth 2H \right) +$$

$$+ 3(b_{23} \coth 3H + 6\kappa \kappa a_{24}) \sigma_1$$

$$q_{32} = a_1 \left[b_{21} \left(\frac{3}{2} - \coth H \coth 2H \right) + \frac{5}{2} \sigma_1 \right] -$$

$$- a_1^2 \left(\frac{11}{8} \coth H - \frac{1}{2} \coth 2H \right)$$

$$q_{33} = 2b_{24} (3 - \coth H \coth 4H) + a_0 (3 + \coth H \coth 2H)$$

$$+ \frac{1}{8} \coth H + \frac{1}{2} a_{24}$$

$$q_{41} = 2\sigma_1 [2(b_{24} \coth 4H + 8\kappa \kappa a_{24}) + a_1^2] +$$

$$+ \frac{3}{2} b_{23} (4 - \coth H \coth 3H)$$

$$q_{42} = 2a_1 [a_2 (3 - \coth^2 H) + a_0 (2 - \coth^2 2H) +$$

$$+ \frac{3}{4} \coth 2H - \frac{1}{8} \coth H] + \frac{1}{2} a_{23}$$

$$q_{51} = 2b_{24} (5 - \coth H \coth 4H) + \frac{1}{2} a_{24} -$$

$$- a_1^2 \left(\frac{3}{8} \coth H - \frac{5}{2} \coth 2H \right)$$

$$q_{52} = 2a_1 \left[a_{23} + \frac{3}{4} b_{23} (5 - 2 \coth 2H \coth 3H) \right]$$

$$b_{30} = \frac{1}{2} [\sigma_1 (1 + 4a_1^2) - b_{21} \coth^2 H]$$

$$- 2a_1 \left[b_{22} \coth^2 2H + \frac{1}{8} (5 \coth H + 2 \coth 2H - a_2) \right]$$

$$b_{3n} = (na_{3n} + \gamma_n)/n, \quad a_{31} = -\sigma_2 + a_2 \coth H \coth 2H$$

$$a_{32} = a_3 + (a_1\sigma_2 + a_2\sigma_1), \quad \sigma_2 = \tau_2 \tau^{-1}$$

REFERENCES

1. Aleshkov, YuZ (1981). "A Theory of Waves at the Surface of Heavy Fluid", Leningrad, Izd LGU, 196pp. (in Russian).
2. Bukatov, AE (1970). "Effect of Ice Cover on Unsteady Waves", Sea Hydrophysical Studies (in Russian: Morskije Gidrofizicheskiye Issledovaniya), Sevastopol, Izd MGI AN USSR, No.3(49), pp.64-77.
3. Bukatov, AE (1994). "Nonlinear Interaction of Surface Waves in a Basin Covered with Broken Ice", Izv. RAN, Ser: Mekh Zhidk i Gaza, No.4, pp.136-143.
4. Bukatov, AE, and Bukatova, OM (1993). "Finite-Amplitude Water Waves in a Basin with Broken Ice", Izv RAN, Ser: Fizika Atm. i Okeana, Vol 29, No.3, pp. 421-425.
5. Bukatov, AE, and Bukatov, AA (1999). "Propagation of Surface Waves of Finite Amplitude in a Basin with Floating Broken Ice", Int J Offshore and Polar Engineering, Vol 9, No.3, pp. 161-166.
6. Bukatov, AE, and Bukatov, AA (2001). "Mass transport under non-linear interaction surface waves in the basin with floating broken ice", Mor Gidrofiz Zhurn, No.2, pp.3-10.
7. Bukatov, AE, and Cherkessov, LV (1971). "Influence of the Ice Cover on the Wave Movement", Sea Hydrophysical Studies (in Russian: Morskije Gidrofizicheskiye Issledovaniya), Sevastopol, Izd. MGI AN USSR, No.2(52), pp.113-144.
8. Il'ichev, AT, and Marchenko, AV (1989). "Propagation of Long Non-linear Waves in a Heavy Liquid Covered with Ice", Izv AN SSSR, Ser: Mekh Zhidk i Gaza, No.1, pp. 88-95.
9. Kheisin, DE (1967). Dynamics of Ice Cover, Leningrad, Gidrometeoizdat, 216 pp. (in Russian).
10. Longuet-Higgins, MS (1987). "Lagrangian Moments and Mass Transport in Stokes Waves", J Fluid Mech, Vol 179, pp. 547-556.
11. Longuet-Higgins, MS (1988). "Lagrangian Moments and Mass Transport in Stokes Waves - Part 2. Water of Finite Depth", J Fluid Mech, Vol 186, pp. 321-336.
12. Nayfeh, AH (1976). Perturbation methods, Moskva, Mir, 455 pp. (in Russian).
13. Nesterov, SV (1968). "Finite-amplitude Wave Generation by a Moving System of Pressures", Izv AN SSSR, Ser: Fizika Atm i Okeana, Vol 4, No.10, pp. 1123-1125.
14. Newman, JN (1985). Marine Hydrodynamics, Leningrad, Sudostroeniye, 367 pp. (in Russian).
15. Peters, AS (1950). "The Effect of a Floating Mat on Water Waves", Comm. Pure Appl. Math, Vol. 3, No.4, pp. 319-354.
16. Phillips, OM (1977). The Dynamics of the Upper Ocean, 2nd. ed, London, Cambridge, Univ. Press, 336 pp.
17. Sretenskii, LN (1936). A Theory of the Fluid Wave Motion, Moskva-Leningrad, ONTI, 296 pp. (in Russian).
18. Stokes, GG (1847). "On the Theory of Oscillatory Waves", Math and Phys Papers, Camb Univ Press, Vol 1, pp. 197-229.
19. Wadhams, P (1986). "The Seasonal Ice Zone", The Geophysics of Sea Ice: Proc NATO Adv. Study Inst. Air-Sea-Ice Interact., New York-London, Plenum Press, pp. 825-991.
20. Weitz, M, and Keller, JB (1950). "Reflection of Water Waves from Floating Ice in Water of Finite Depth", Comm. Pure Appl. Math, Vol.3, No.3, pp. 305-318.